

Table of Contents

摘 要	I
Abstract	II
誌 謝	IV
Table of Contents	V
List of Figures	VII
List of Tables	XI
Chapter 1 Introduction	1
1.1 Motivation.....	1
1.2 Related Researches	2
1.2.1 Fabrication of Microlens.....	2
1.2.2 Fabrication of Aperture.....	5
1.2.3 Integrated MO Structure	9
1.3 Current Approach.....	12
Chapter 2 Principle and Design	14
2.1 Basic Near-Field Recording (NFR) Principle.....	14
2.2 MO Recording Theorem	16
2.3 Concept Design.....	18
2.4 Self-Alignment Concept	20
2.5 Designs of Individual Parts.....	21
2.5.1 Sub-Micro Aperture	21
2.5.2 The Solid Immersion Lens (SIL)	24
Chapter 3 Fabrication	28
3.1 General Fabrication Flow-Chart	29

3.2 Fabrication in Self-Alignment Process	35
3.3 Process of Sub-micro Aperture Fabrication.....	37
3.4 Process of SIL Fabrication.....	43
3.4.1 Basic Theory of Thermal Reflowing	44
3.4.2 Fabrication of SIL	45
3.5 Process of Microcoil/Pad Fabrication.....	52
3.6 Integration Structure of NFR Pick-up Head	55
Chapter 4 Simulation and Measurement.....	58
4.1 Simulation.....	58
4.1.1 Fiberlens.....	59
4.1.2 Fiberlens and SIL.....	60
4.2 Measurement.....	62
4.2.1 Principle	63
4.2.2 Experiment Setup.....	65
4.2.3 Self-Alignment Verification.....	68
4.2.4 Spot Size Calibration	69
4.2.5 SIL Reliability.....	72
Chapter 5 Summary	75
5.1 Discussion.....	75
5.2 Conclusion	76
Reference.....	78



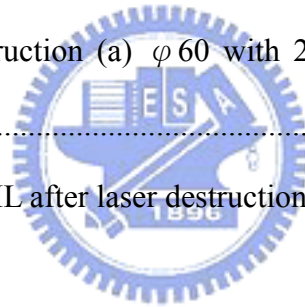
List of Figures

Fig.1-1 Fabrication process of Si microlens by selective etching	2
Fig.1-2 Fabrication of the SIL by press molding	3
Fig.1-3 Schemes of microlens arrays fabrications	3
Fig.1-4 Fabrication process of microlens array	4
Fig.1-5 Fabrication of a fiber tip by chemical etching.....	5
Fig.1-6 Exposure by using the Evanescent Wave	5
Fig.1-7 Fabrication of a metallic aperture by using FIB milling	6
Fig.1-8 Scheme of the fabrication process of a aperture	6
Fig.1-9 Making a sub-micro aperture by over-electroplating	7
Fig.1-10 Fabrication process for aperture array combined with the SIL.....	8
Fig.1-11 Batch fabrication process to combine the SIL and aperture.....	8
Fig.1-12 MO pick-up head combined the SIL, microcoil.....	10
Fig.1-13 Cross section of the near-field optical pick-up head	10
Fig.1-14 (a) Schematic drawing of a micro optical pick-up head composed of the objective lens, focusing actuator, microcoil, and air-bearing (b) the air-bearing structure	11
Fig.1-15 Near-field optical pick-up head structure	12
Fig.2-1 Illustration of a lens to focus the incident light.....	14
Fig.2-2 Principles of the SIL and SSIL (Tsai, 1998).....	15
Fig.2-3 (a) The basic theorem of MO recording (b) The material of recording disk... 16	16
Fig.2-4 Intensity distribution of the laser beam with and without the sub-micro aperture	18
Fig.2-5 Integrated MO pick-up head structure	19
Fig.2-6 (a) The Self-Alignment mechanism (b) The thermal reflowing mechanism ..	21

Fig.2-7 (a) Initial aperture size defined into a pedestal layer (b) Aperture size after shrinking with metal deposited (c) The basic geometrical for aperture design	22
Fig.2-8 Standard structure (a) SSIL (b) SIL.....	24
Fig.2-9 Absorption versus thickness of the AZ-4620	24
Fig.2-10 The parameters of the fabricated SIL structure	25
Fig.2-11 The aspect ratio of the patterned photoresist is (a) Small than 3/5 for the SIL structure (b) Large than 3/5 for the SSIL structure	26
Fig.2-12 The profile of photoresist pattern after thermal reflowing process	26
Fig.3-1 The total MO pick-up head structure	29
Fig.3-2 The general fabrication flowchart of MO pick-up	33
Fig.3-3 Initial aperture 4 μ m and opening ring pattern (a) Photoresister FH6400 pattern (b) After lift-off process (c) After undercutting process	38
Fig.3-4 The photoresister ring pattern in initial aperture boundary before reflowing .	39
Fig.3-5 (a) A slope sidewall in initial aperture boundary after reflowing (b) The aperture with diameter of 2.88 μ m.....	40
Fig.3-6 The photoresister AZ4620 pattern for shrinkage initial aperture (a) The lateral view (b) The top view	40
Fig.3-7 The diameter of aperture (a) before shrinkage process with 4.55 μ m (b) after shrinkage process with 4.05 μ m.....	42
Fig.3-8 (a) The view of sputtering equipment (b) The gun of target and wafer holder	43
Fig.3-9 Illustration of profile change before and after thermal reflow process	44
Fig.3-10 Backside exposure mechanism.....	46
Fig.3-11 The fabrication result of PR AZ-4620 thickness	47
Fig.3-12 The diameter of columnar pattern AZ-4620 is (a) 58.57 μ m (b) 68.26 μ m	47
Fig.3-13 (a) The result of backside exposure (b) the diffraction phenomenon in	

backside exposure step.....	48
Fig.3-14 The fabrication results of SIL (a) before reflowing (b) after reflowing	49
Fig.3-15 The 3-D profile measuring results of SIL of diameter (a) 60 μ m (b) 70 μ m...50	
Fig.3-16 The 2-D curve measuring results of SIL of diameter (a) 60 μ m (b) 70 μ m	50
Fig.3-17 The real surface profile data of SIL of diameter (a) 60 μ m (b) 70 μ m.....	50
Fig.3-18 The SIL of diameter after reflowing with (a) 56.26 μ m (b) 66.92 μ m.....	51
Fig.3-19 The illustration of exposer equipment.....	52
Fig.3-20 (a) The PR pattern for Cu seed lift-off (b) The Cu seed pattern after lift-off	53
Fig.3-21 (a) The PR mold for electroplating (a) Ni microcoil/pad after electroplating	53
Fig.3-22 (a) Illustration of the electroplating equipment (b) The structure of solution tank (c) Wafer holder and conductive wire.....	55
Fig.3-23 (a) Fabrication results of aperture and microcoil/pad (b) an aperture in NFR pick-up head.....	56
Fig.3-24 The fabrication results of (a) backside exposure step (b) thermal reflowing	57
Fig.4-1 All components and variables in simulation condition	58
Fig.4-2 The fiberlens simulation setup	59
Fig.4-3 Fiberlens length vs. Spot size and NA	59
Fig.4-4 Refraction index of AZ-4620 20 μ m versus thermal reflowing time at 150 $^{\circ}$ C	60
Fig.4-5 The simulation setup of fiberlens combining the SIL component	61
Fig.4-6 A co-focal system in measurement setup	62
Fig.4-7 Definition of output beam size	63
Fig.4-8 Focusing a beam with a lens at the beam waist.....	64
Fig.4-9 Focusing a collimated beam.....	65
Fig.4-10 Illustration of the fiberlens measuring system	66
Fig. 4-11 Illustration of the fiberlens with SIL/aperture component measuring system	

.....	67
Fig.4-12 Intensity of ambient.....	68
Fig.4-13 The measurement result of self-alignment verification.....	69
Fig.4-14 Photograph of fiberlens with radius 62.5 μm	69
Fig.4-15 The beam profile of fiberlens with 2.99 μm spot size.....	70
Fig.4-16 The beam profile of fiberlens with aperture/ φ 60 SIL with 2.09 μm spot size	71
Fig.4-17 The beam profile of fiberlens with aperture/ φ 70 SIL with 2.12 μm spot size	71
Fig.4-18 SIL before laser destruction (a) φ 60 with 2.02 μm spot size (b) φ 70 with 2.08 μm spot size	73
Fig.4-19 SIL after laser destruction (a) φ 60 with 2.01 μm spot size (b) φ 70 with 2.12 μm spot size	73
Fig.4-20 The photograph of SIL after laser destruction.....	74



List of Tables

Tab.2-1 The design parameters of aperture.....	23
Tab.2-2 The design parameters of SIL.....	27
Tab.3-1 Fabrication in self-alignment process.....	36
Tab.3-2 The parameters of physical sputtering (DC gun only).....	41
Tab.3-3 The parameters of physical sputtering (DC and RF gun).....	42
Tab.3-4 Parameters of photolithography.....	43
Tab.3-5 The designed parameters and fabrication results of surface profile of SIL.....	51
Tab.3-6 Parameters of photolithography.....	52
Tab.3-7 Parameters of electroplating process.....	54
Tab.3-8 Basic electroplating theories.....	54
Tab.4-1 The parameters of SIL size.....	60
Tab.4-2 The refractive indexes in simulation condition setting.....	61
Tab.4-3 The simulation results of fiberlens combining SIL.....	61
Tab.4-4 Specification of CCD camera.....	68
Tab.4-5 The simulation and measurement results of spot size.....	72